ChemComm

Accepted Manuscript

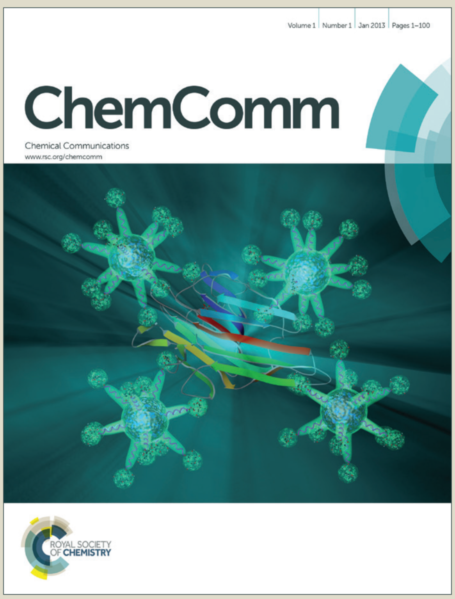

Cite this: DOI: 10.1039/c0xx00000x

www.rsc.org/xxxxxx

ARTICLE TYPE

Highly Stable Covalent Organic Framework-Au Nanoparticles Hybrids for Enhanced Activity for Nitrophenol Reduction

Pradip Pachfule,[a] Sharath Kandambeth,[a] David Díaz Díaz,[b,c] and Rahul Banerjee[a]*

Received (in XXX, XXX) Xth XXXXXXXXX 20XX, Accepted Xth XXXXXXXXX 20XX
DOI: 10.1039/b000000x

Gold [Au(0)] nanoparticles immobilized into stable covalent organic framework (COF) has been synthesized *via* solution infiltration method. As-synthesized Au(0)@TpPa-1 catalyst shows superior reactivity and high recyclability for nitrophenol reduction reaction than $HAuCl_4.3H_2O$.

Covalent organic frameworks (COFs) are lightweight and porous materials well known for their applications in gas storage, catalytic supports, semiconductive and photoconductive devices.[1] In addition to the other porous materials *viz.* charcoal, dendrimers, polymers, mesoporous silica, zeolites, MOFs, etc.; metal doped COFs have also been practised as catalysts for organic reactions.[2] Although, well ordered periodicity and high surface area of COFs facilitated the usages of these materials as catalyst support, the stability of host COF supports in aqueous/acidic/alkaline reaction mediums still remains a crucial aspect for using the same catalyst over number of cycles.[3] Despite the limited surface area of COFs, nanoparticles@COFs has been used as catalyst for Suzuki coupling, C–H activation, Knoevenagel condensation, nitro reduction, glycerol oxidation, etc.[4] Since, the COF based supports used to decorate the nanoparticles are unstable in aqueous and most of the organic solvents, tedious synthetic protocols are followed for the synthesis as well as usages of these catalysts in aforementioned reactions.[5] Moreover, the concerns regarding sintering, leaching, stability and recyclability of supported nanoparticles in diverse reaction conditions remain at the forefront.[6] Thus, in order to overcome these issues regarding the optimal interaction, we believe that the synthesis of new materials having strong interactions between support and loaded nanoparticles with high stability in aqueous/acidic/alkaline mediums is desired.

Gold (Au) nanoparticles decorated on suitable supports hold unique advantages as heterogeneous catalyst under mild conditions, even at ambient temperature with high reaction rates.[7] Although, there are reports of host supported Au catalysts which showed high catalytic activity for oxidations, hydrogenation, cyclization, rearrangement, C−C coupling reactions, etc.; the unstable supports holding these nanoparticles brings limitations to their uses.[8] Most importantly, the weak interactions between supports and nanoparticles usually results into sintering and leaching of nanoparticles. In these regards, Au catalysts supported on carbon, CeO_2, Al_2O_3, Fe_2O_3, etc. has been used as catalysts for the hydrogenation of environmental pollutant 4-nitrophenol (4-NPh), which is anthropogenic, toxic and inhibitory in nature; to yield industrially important anilines like 4-aminophenol.[2a,8c] Since, 4-aminophenol (4-APh) is important due to its usages as a developer in black and white films and intermediate for the synthesis of drug Paracetamol; for its synthesis, a catalytic system with high associated product yield, selectivity and recyclability is desirable. In order to simplify the modus operandi, herein for the first time, we report a simple synthetic route to acquire a highly stable, porous and crystalline COF (**TpPa-1**) supported Au nanoparticles hybrids *via* solution infiltration method.[9] Herein, along with synthesis of robust and stable **Au(0)@TpPa-1** catalyst, the catalytic activities of synthesized catalyst towards 4-nitrophenol (4-NPh) reduction have been illustrated.

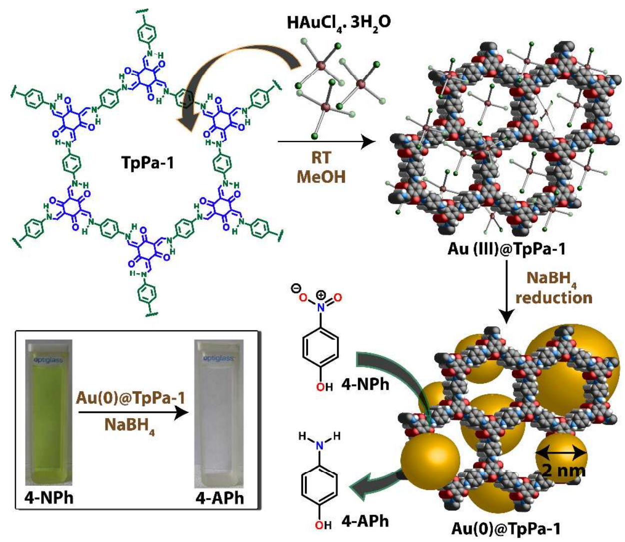

Scheme 1. Synthesis of **Au(0)@TpPa-1** catalyst using solution infiltration method for nitrophenol reduction reaction. Inset image: The optical images of the color change observed for the conversion of 4-nitrophenol to 4-aminophenol after the addition of **Au(0)@TpPa-1**.

As shown in scheme 1, **Au(0)@TpPa-1** catalyst was synthesized by mixing **$HAuCl_4$. $3H_2O$** (1.5 mg, 0.004 mmol) with evacuated **TpPa-1** (98.5 mg) in 5 ml methanol, under vigorous stirring.[9] From the obtained mixture, solvent was removed by evacuation and subsequently 3 ml methanol was added. To this solution, 2 ml of 0.5 mmol (20 mg) $NaBH_4$ solution in methanol was added with stirring, and the obtained mixture was dried under vacuum after washing to obtain **Au(0)@TpPa-1** catalyst (ESI, Section S3). The consequential

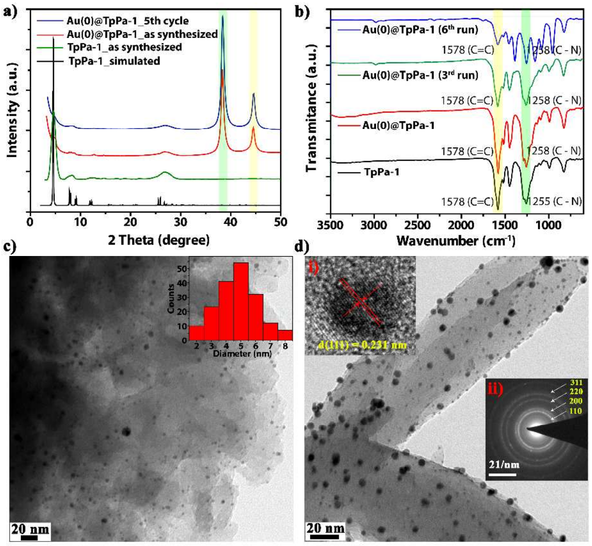

Fig. 1: a) PXRD profile of **Au(0)@TpPa-1**. Matching PXRD plots of **TpPa-1**, **Au(0)@TpPa-1** and **Au(0)@TpPa-1** after 3rd and 5th catalytic cycle. b) Comparison of the FT-IR spectra of **Au(0)@TpPa-1** with **TpPa-1,** catalyst recovered after 3rd and 6th run. c) Low resolution TEM image of **Au(0)@TpPa-1**. Inset image: Nanoparticles size distribution histogram. d) High resolution TEM image of **Au(0)@TpPa-1**. Inset images: i) Single Au nanoparticle showing d-spacing, ii) The corresponding SAED pattern.

feature of the reported **Au(0)@TpPa-1** catalyst having high stability in aqueous and common organic solvents is associated with the proper selection of support chosen as stable COF (**TpPa-1**) having well ordered porous architecture enriched with oxygen and nitrogen containing crystalline framework, which provides extra strength to the nanoparticles. Here, the stability of synthesized catalyst was assumed to be optimal, since the **TpPa-1** has the stability in aqueous, acidic as well as alkaline medium.

The well maintained PXRD patterns of **Au(0)@TpPa-1** with additional peaks for (111) and (200) planes appearing ~39° (2θ) and ~44° (2θ) than **TpPa-1**, demonstrated the successful loading of Au nanoparticles with retention of the COF integrity and minimal loss of crystallinity as shown in Fig. 1a. The presence of all characteristics peaks of **TpPa-1** in the FT-IR spectrum of **Au(0)@TpPa-1** confirmed that, even after strong treatment with $NaBH_4$, the chemical composition within the COF framework remained intact (Fig. 1b). After incorporation of Au(0) nanoparticles inside the **TpPa-1** template, the appearance of strong representative peaks for C=C (~1578 cm^{-1}) and C–N (~1258 cm^{-1}) stretching of **TpPa-1**, confirmed the metal loading without disturbing the basic **TpPa-1** architecture. The complete reduction of Au(III) to Au(0) in presence of excess $NaBH_4$ was confirmed from the X-ray photoelectron spectroscopy (XPS) analysis (ESI, Fig. S9). The extent of Au nanoparticle loading on **TpPa-1** was further confirmed by the decreased N_2 adsorption and BET surface area of **Au(0)@TpPa-1** (339 m^2/g) in comparison with as synthesized **TpPa-1** (484 m^2/g). As the pore surface (partially or fully) and interlayer spacings in the host COF framework are occupied by finely dispersed Au(0) nanoparticles located at the surface as well as inside the COF matrix, the observed decrease in BET surface area and pore size is justified (ESI, Fig. S7, S8). From the EDAX, ICP and TGA analysis performed for **Au(0)@TpPa-1**, the loading of ~1.2 wt% of Au nanoparticles on **TpPa-1** was confirmed (ESI, Fig. S6, S19).

As the morphological factors of the supported nanoparticles contribute into the actual reactivity and recyclability of catalysts, we have performed the SEM and TEM analyses of the synthesized catalyst.[10] The flower like morphology of the pristine **TpPa-1** was observed to be maintained to some extent even after the loading of Au(0) nanoparticles (ESI, Fig. S2, S4). The micrometer sized petals of **TpPa-1** observed into the SEM analysis found to be the aggregation of the few sheet like structures from the TEM analysis, which serves as host for the doped nanoparticles (Fig. 1d; ESI, Fig.S3). The loading of finely distributed, 5±3 nm sized Au(0) nanoparticles was clearly visible in TEM analyses performed for **Au(0)@TpPa-1** (Fig. 1c), in concurrence with the particle size calculated from the observed PXRD patterns using Scherrer Equation . The 3D loading of these nanoparticles throughout the matrix of **TpPa-1** was clearly perceptible from dark field TEM imaging of the **Au(0)@TpPa-1** (Fig. S5). The interplanar d-spacing (0.231 nm) in the lattice fringes indicates the formation of Au(0) -nanoclusters oriented in the (111) plane (Fig. 1d; inset i). The SAED pattern reveals the growth of nanocrystals with (200) and (220) orientations, with the presence of nanocrystalline texture in agreement with the observed XRD patterns (Fig. 1d; inset ii).

Since, we have observed uniform loading of 5±3 nm sized Au nanoparticles on **TpPa-1** matrix with fine dispersion; we evaluated the kinetic as well as energetic parameters of well known nitrophenol reduction reaction using **Au(0)@TpPa-1** catalyst. In order to confirm the heterogeneity of the catalyst, we have carried out standard leaching experiment using **Au(0)@TpPa-1** catalyst, which confirmed the stable loading of Au nanoparticles on **TpPa-1** in water as well as common organic solvents (ESI, Fig. S16). The strong interaction of Au nanoparticles with **TpPa-1** proves that the heterogeneity of the catalyst remains intact in standard catalytic conditions. As synthesised **Au(0)@TpPa-1** were tested for the catalytic reduction of 4-NPh in presence of excess $NaBH_4$ in water as solvent. The reduction kinetics was monitored by UV-vis absorption spectroscopy of the reaction mixture after the addition of the catalyst. As the reaction proceed, the absorbance of 4-NPh at ~400 nm start decreasing along with a related increase in the ~300 nm peak corresponding to 4-aminophenol (4-APh). The reaction did not occur when using only TpPa-1 as the catalyst and proceeded comparatively slower with $HAuCl_4 \cdot 3H_2O$ (conversion time: 20 min) and Au(0)@TpPa-1 (2.20 wt%, conversion time: 18 min) as catalysts (Section S4). When, 1.2 wt% Au loaded **Au(0)@TpPa-1** catalyst has been used as catalyst, the significant catalytic activity was observed and conversion of 4-NPh to 4-APh was seen to be completed within 13 min. The probable reason of the momentous activity shown by **Au(0)@TpPa-1** (1.20 wt%) over **Au(0)@TpPa-1** (2.20 wt%) may be the fine distribution of very tiny nanoparticles (5±3 nm) on the **TpPa-1** matrix, which lead to a very large surface area of the nanoparticles and high particle number per unit mass for the catalyst. The increased fraction of the atoms at the surface in **Au(0)@TpPa-1** leads to significantly higher catalytic activity.

In view of the fact that the concentration of BH_4^- added in the system is excess compared to the concentration of 4-NPh, it is assumed that the concentration of BH_4^- remains constant during

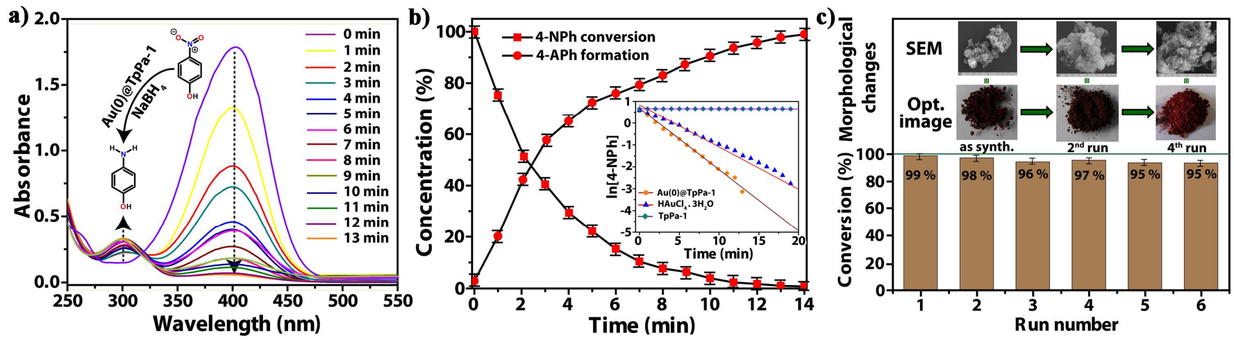

Fig. 2. a) Typical time-dependent evolution of UV–Vis spectra showing the catalytic reduction of 4-NPh to 4-APh by **Au(0)@TpPa-1**. b) Kinetics of the reduction reaction of 4-NPh to 4-APh. Inset Image: Plots of ln[4-NPh] of absorbance of 4-nitrophenol at 400 nm obtained from (a) versus time for the reduction of 4-nitrophenol catalyzed by **Au(0)@TpPa-1**, **HAucl$_4$. 3H$_2$O** and **TpPa-1**. c) Conversion of 4-NPh in 6 cycles of reaction by **Au@TpPa-1** catalyst. Inset image: Morphological changes observed in **Au(0)@TpPa-1** catalyst with increasing number of cycles traced by optical imaging and SEM.

the reaction. In this circumstance, pseudo-first-order kinetics has been used to evaluate the kinetic reaction rate of the catalytic reaction (Fig. 2b, inset). Herein, a linear correlation of ln[4-NPh] versus time at any instant is obtained. Among all the tested catalysts for 4-NPh reduction, **Au(0)@TpPa-1** (1.20 wt%) has the highest activity with a rate constant of ~5.35×10^{-3} s^{-1}. The sluggish reaction kinetics in presence of **HAuCl$_4$.3H$_2$O** (~3.01×10^{-3} s^{-1}) than that of **Au(0)@TpPa-1** highlights the utility of supported nanoparticles for catalyzing organic transformation reactions heterogeneously (Fig. 2c). This catalytic activity is superior than well known Au and Ag based catalysts tested under similar conditions (ESI, Table S1).[11] Additionally, the catalyst has also showed excellent recyclability for more than 6 catalytic cycles giving yields over 95 % in estimated time span of 13 min. As calculated by the Arrhenius equation (Fig. S15), the rate of 4-NPh reduction increased with temperature. The stability of the catalyst after catalytic cycles was furthermore confirmed by the optical, SEM, TEM imaging of the catalyst recovered after catalytic runs (Fig. 2c inset; ESI, Fig. S17, S18). The FT-IR and PXRD analyses of reused catalyst once again highlights the stability and crystallinity of the COF support holding the nanoparticles intact even after used for 6 cycles (Fig. 1a, 1b). Moreover, as shown in the Figure S14, the non-aggregation of nanoparticles in the reused catalyst further confirms the stability of the prepared catalysts. Hence, it can be confirmed that the prominent catalytic activity of **Au(0)@TpPa-1** might be assigned to the highly stable, two dimensional support (**TpPa-1**) which holds the loaded nanoparticles to high extent.

In summary, for the first time, we have synthesized a COF-supported highly stable Au(0) based catalyst via solution infiltration methods, which shows a high activity towards nitrophenol reduction reaction. The synthesized **Au(0)@TpPa-1** catalyst shows superior reactivity for nitrophenol reduction reaction than **HAuCl$_4$.3H$_2$O** imparting the advantages of heterogeneous catalysts. The phenomenon of maintaining crystallinity over number of cycles is very rare in literature and herein we have demonstrated the usefulness of stable and crystalline support for the improved catalytic activity. The overall recyclability with almost unchanged reactivity for more than 6 cycles shown by the reported catalyst is promising towards the heterogenization of Au catalyst for commercially important transformation reactions.

RB and PP acknowledges CSIR (CSC0102 and CSC0122) for funding.

Notes and references

[a] *Physical/Materials Chemistry Division, CSIR-National Chemical Laboratory, Dr. Homi Bhabha Road, Pune 411008, India; Tel: +912025902535; E-mail: r.banerjee@ncl.res.in*

[b,c] *Institut für Organische Chemie, Universität Regensburg, Universitätsstr. 31, 93053 Regensburg (Germany) and IQAC-CSIC (Spain).*

† Electronic Supplementary Information (ESI) available: Experimental procedures, IR, Gas adsorption and additional supporting data. See DOI: 10.1039/b000000x/

1 (*a*) K. Sakaushi, E. Hosono, G. Nickerl, T. Gemming, H. Zhou, S. Kaskel, J. Eckert, *Nat. Commun.* 2013, **4**, 1485; (b) M. Dogru and T. Bein, *ChemComm,* 2013, **DOI:** 10.1039/C3CC46767H. (*c*) J. W. Colson and W. R. Dichtel, *Nat. Chem.* 2013, **5**, 453; (*d*) X. Feng, X. Ding, D. Jiang, *Chem. Soc. Rev.* 2012, **41**, 6010; (*e*) C. J. Doonan, D. J. Tranchemontagne, T. G. Glover, J. R. Hunt and O. M. Yaghi, *Nat. Chem.,* 2010, **2**, 235.
2 (*a*) A. Corma and H. Garcia, *Chem. Soc. Rev.* 2008, **37**, 2096; (*b*) J. C. Fierro-Gonzalez and B. C. Gates, *Chem. Soc. Rev.* 2008, **37,** 2127.
3 (*a*) S. Proch, J. Herrmannsdörfer, R. Kempe, C. Kern, A. Jess, L. Seyfarth, L. Senker, *Chem. Eur. J.* 2008, **14**, 8204. (*b*) T. Ishida, M. Nagaoka, T. Akita, M. Haruta, *Chem. Eur. J.* 2008, **14**, 8456.
4 (*a*) C. E. Chan-Thaw, A. Villa, P. Katekomol, D. Su, A. Thomas and L. Prati, *Nano Lett.* 2010, **10**, 537; (*b*) S.-Y. Ding, J. Gao, Q. Wang, Y. Zhang, W.-G. Song, C.-Y. Su and W. Wang, *J. Am. Chem. Soc.* 2011, **133**, 19816; (*c*) S. B. Kalidindi, K. Yusenko and R. A. Fischer, *Chem. Commun.* 2011, **47**, 8506; (*d*) P. Zhang, Z. Weng, J. Guo and C. Wang, *Chem. Mater.* 2011, **23**, 5243; (*e*) Y. Zhou, Z. Xiang, D. Cao and C.-J. Liu, *Chem. Commun.* 2013, **49**, 5633.
5 (*a*) J. Long, H. Liu, S. Wu, S. Liao, Y. Li, *ACS Catal*. 2013, **3**, 647. (*b*) S. B. Kalidindi, H. Oh, M. Hirscher, D. Esken, C. Wiktor, S. Turner, G.V. Tendeloo, R.A. Fischer, *Chem. Eur. J.* 2012, **18**, 10848.
6 P. Forzatti, L. Lietti, *Catal. Today* 1999, **52**, 165.
7 (*a*) D. J. Cole-Hamilton, *Science*, 2003, **299**, 1702; (*b*) P. Hervés, M. Pérez-Lorenzo, L. M. Liz-Marzán, J. Dzubiella, Y. Lu and M. Ballauff, *Chem. Soc. Rev.*, 2012, **41**, 5577.
8 (*a*) F. Zaera, *Chem. Soc. Rev.*, 2013, **42**, 2746; (*b*) S. Schauermann, N. Nilius, S. Shaikhutdinov and H.-J. Freund, *Acc. Chem. Res.*, 2013, **46**, 1673; (*c*) A. Corma and P. Serna, *Science*, 2006, **313**, 332.
9 S. Kandambeth, A. Mallick, B. Lukose, M. V. Mane, T. Heine and R. Banerjee, *J. Am. Chem. Soc.* 2012, **134**, 19524.
10 a) A. T. Bell, *Science* 2003, **299**, 1688; b) M. S. Chen and D. W. Goodman, *Catal. Today,* 2006, **111**, 22.
11 (*a*) K. Hayakawa, T. Yoshimura and K. Esumi, *Langmuir*, 2003, **19**, 5517; (*b*) Y. Lu, Y. Mei, M. Drechsler and M. Ballauff, *Angew. Chem. Int. Ed.*, 2006, **45**, 813; (*c*) S. Jana, S. K. Ghosh, S. Nath, S. Pande, S. Praharaj, S. Panigrahi, S. Basu, T. Endo and T. Pal, *Appl. Catal.* A, 2006, **313**, 41; (*d*) J. Lee, J. C. Park and H. Song, *Adv. Mater*. 2008, **20**, 1523.